

1 **Title**

2 Sensitive detection of SARS-CoV-2 seroconversion by flow cytometry reveals the presence
3 of nucleoprotein-reactive antibodies in unexposed individuals

4 **Authors and affiliations**

5 Leire Egia-Mendikute^{1,†}, Alexandre Bosch^{1,†}, Endika Prieto-Fernández¹, So Young Lee¹,
6 Borja Jiménez-Lasheras¹, Ana García del Río¹, Asier Antoñana-Vildosola¹, Chiara
7 Bruzzone², Mainer Bizkarguenaga², Nieves Embade², Rubén Gil-Redondo², María Luz
8 Martínez-Chantar^{3,4}, Marcos López-Hoyos⁵, Nicola G A Abrescia^{4,6,7}, Jose M. Mato^{2,4}, Oscar
9 Millet², Asís Palazón^{1,7,*}

10 ¹Cancer Immunology and Immunotherapy Lab, CIC bioGUNE, Basque Research and
11 Technology Alliance (BRTA), 48160, Bizkaia, Spain.

12 ²Precision Medicine and Metabolism Lab, CIC bioGUNE, Basque Research and Technology
13 Alliance (BRTA), 48160, Bizkaia, Spain

14 ³Liver Disease Laboratory, CIC bioGUNE, Basque Research and Technology Alliance
15 (BRTA), 48160, Bizkaia, Spain.

16 ⁴Centro de Investigación Biomédica en Red de Enfermedades Hepáticas y Digestivas
17 (CIBERehd), Instituto de Salud Carlos III, 28029, Madrid, Spain.

18 ⁵Servicio Inmunología, Hospital Universitario Marqués de Valdecilla-IDIVAL, Facultad de
19 Medicina, Universidad de Cantabria, 39008 Cantabria, Spain.

20 ⁶Structure and Cell Biology of Viruses Lab, CIC bioGUNE, Basque Research and
21 Technology Alliance (BRTA), 48160, Bizkaia, Spain.

22 ⁷Ikerbasque, Basque Foundation for Science, 48015, Bizkaia, Spain.

23 *Correspondence: apalazon@cicbiogune.es

24 [†]These authors contributed equally.

25 **Abstract**

26 There is an ongoing need of developing sensitive and specific methods for the determination
27 of SARS-CoV-2 seroconversion. For this purpose, we have developed a multiplexed flow
28 cytometric bead array (C19BA) that allows the identification of IgG and IgM antibodies
29 against three immunogenic proteins simultaneously: the spike receptor-binding domain
30 (RBD), the spike protein subunit 1 (S1) and the nucleoprotein (N). Using different cohorts of
31 samples collected before and after the pandemic, we show that this assay is more sensitive
32 than ELISAs performed in our laboratory. The combination of three viral antigens allows for
33 the interrogation of full seroconversion. Importantly, we have detected N-reactive antibodies
34 in COVID-19-negative individuals. Here we present an immunoassay that can be easily
35 implemented and has superior potential to detect low antibody titers compared to current
36 gold standard serology methods.

37 **Introduction**

38 The severe acute respiratory syndrome coronavirus 2 (SARS-CoV-2) global spread has
39 resulted in an ongoing pandemic¹. To date, most immunoassays to determine
40 seroconversion and measure antibody responses are based on enzyme-linked
41 immunosorbent assay (ELISA), including automated chemiluminescent variants. Serological
42 assays are important to detect previously infected individuals and perform epidemiological
43 seroconversion studies²⁻⁴. Moreover, they have important implications in the development of
44 antibody-based therapeutics (i.e. convalescent serum or monoclonal antibodies) and
45 vaccines (i.e. selection of non-immunised individuals and follow-up). For these reasons,
46 there is a need of developing fast and sensitive serology assays that can be deployed at a
47 large scale⁵.

48 SARS-CoV-2 contains several structural proteins, among them the Spike (S) and the
49 Nucleoprotein (N) are the most immunogenic viral antigens and are used in serologic
50 assays^{6,7}. The S protein is comprised of two subunits: S1 and S2. S1 includes the receptor-
51 binding domain (RBD) that binds to its cognate receptor angiotensin converting enzyme 2
52 (ACE2) expressed by host cells⁸⁻¹⁰. Its sequence is specific for SARS-CoV-2, often
53 generating neutralizing antibodies in seropositive individuals¹¹. Given their specificity, both
54 RBD and S are considered ideal for serology assays¹²⁻¹⁴, especially in the form of
55 recombinant proteins produced in mammalian cell systems that reflect a physiological
56 glycosylation pattern¹⁵. Humoral immunity against SARS-CoV-2 has been reported¹⁶,
57 including the presence of neutralizing antibodies in seropositive individuals¹⁷. Moreover,
58 specific cellular responses have been described, including memory T cell formation against
59 immunodominant peptides¹⁸⁻²⁰.

60 In general, ELISAs have an acceptable specificity and sensitivity profile for performing large
61 epidemiological studies, but their sensitivity in the context of SARS-CoV-2 serology could be
62 improved^{21,22}. A key limitation of ELISA is the need of individual plates/wells for each antigen
63 or antibody class to be tested. Moreover, the antigen is immobilised to the plate, which can

64 hide epitopes or increase the background noise. For these reasons, ELISAs are not well
65 suited to detect low antibody titers and often give undetermined values that are close to the
66 cut-off, leading to difficult interpretation of results.

67 Cytometric bead arrays offer an alternative to perform serology. This technology allows for
68 the rapid identification of multiple analytes simultaneously on a multiplexed manner,
69 requiring less amounts of sample than traditional immunoassays²³. Its reproducibility and
70 sensitivity are well characterised, especially for measuring cytokines²⁴. The readout is based
71 on flow cytometry, open systems that are widely available in clinical and research settings.

72 In this study, we have developed a flow-cytometric bead array (C19BA) to assess
73 seroconversion against SARS-CoV-2, leveraging the multiplex capability of this technology
74 for the simultaneous interrogation of the presence of IgG and IgM antibodies against three
75 viral antigens. This approach unravelled the presence of N-reactive antibodies in a cohort of
76 samples collected before the pandemic, indicating that cross-reactivity against this
77 conserved viral protein exists.

78 **Results**

79 **Development of a flow cytometric bead array (C19BA) for the detection of SARS-CoV-**
80 **2 seroconversion**

81 The presented flow cytometry assay consists in a multiplexed array containing microbeads
82 with different intrinsic fluorescence intensities coated with viral antigens. The coupling was
83 performed with microbeads functionalized with streptavidin and proteins tagged with a
84 unique terminal biotin, which allows for the orientation of the antigen on the surface of the
85 bead. The bead array (C19BA) is incubated with serum samples to allow the binding of anti-
86 SARS-CoV-2 antibodies and then stained with anti-IgG and anti-IgM secondary antibodies
87 labelled with different fluorochromes (Figure 1A). In order to fully assess the specific
88 seroconversion against SARS-CoV-2, we have chosen RBD, S1 and N as target antigens.
89 The redundancy of RBD as a sequence included in S1 allows for the confirmation of intra-
90 assay specificity on different microbeads simultaneously. The N protein was also included in
91 the assay because of its immunogenicity. N is predicted to be less specific for SARS-CoV-2
92 based on the analysis of the sequence alignment with other coronavirus family members
93 (Supplementary Figure 1). We reasoned that fully seroconverted individuals would present
94 antibodies against the three chosen antigens. C19BA includes uncoated negative control
95 beads and positive control beads that are coated with human IgG and IgM (Figure 1B). This
96 setup differentiates each type of microbead as shown in the non-overlapping histograms in
97 Figure 1C. We first tested the ability of this assay to identify recombinant IgG antibodies
98 against RBD and N. As can be seen on Figure 1D, the microbead array clearly identified the
99 binding of these antibodies. Importantly, the sensitivity of C19BA was superior to the ELISA
100 presented here (Figure 2) when their performance was compared in serial dilutions of
101 commercial anti-RBD and anti-N IgG antibodies. C19BA presented a better broader dynamic
102 range and identified low antibody concentrations that were not detected by ELISA.

103 **Determination of SARS-CoV-2 seroconversion on preCOVID-19 and acute COVID-19**
104 **cohorts by C19BA**

105 We then applied C19BA to interrogate serum samples from a cohort of 43 individuals who
106 tested positive for SARS-CoV-2 infection by polymerase chain reaction (PCR). These
107 samples were obtained at the time of hospital admission (acute COVID cohort). As a control,
108 sera from 50 individuals collected before the pandemic (2018-2019) were analysed
109 (preCOVID cohort). Both ELISA and C19BA were able to discriminate both cohorts based on
110 the presence of IgG and IgM antibodies against RBD, S1 and N. At this early stage of
111 infection, not all samples from the acute COVID cohort presented reactivity against viral
112 antigens (Supplementary Figure 2). Serial dilutions of 10 seropositive acute COVID and 10
113 preCOVID samples were performed to further compare the sensitivity of C19BA versus
114 ELISA. Figure 3A shows the dilution curves corresponding to the presence of IgG antibodies
115 by these two methods. C19BA was superior to the ELISA presented here separating both
116 cohorts and identifying the presence of antibodies at lower concentrations. This was
117 confirmed by plotting the area under the curve (AUC) and determining its statistical
118 significance (Figure 3B). The titers of IgM antibodies were lower than IgG as measured by
119 both methods (Figure 3C-D), in line with previous studies¹⁶. Importantly, our assay identified
120 the presence of N-reactive IgG antibodies in 6 preCOVID samples (n=50), although in
121 general at lower titers than in the acute COVID cohort (Figure 3A-B). Figure 4 shows
122 representative dot plot profiles corresponding to preCOVID and COVID samples. While the
123 reactivity against RBD and S1 was specific for COVID samples, cross-reactivity against N
124 was observed in some preCOVID individuals that contained IgG, but not IgM antibodies. No
125 cross-reactivity against SARS-CoV-2 RBD or S1 was observed on serum samples that
126 tested seropositive against the spike of other common cold coronaviruses (Supplementary
127 Figure 3). In the acute COVID cohort, several samples that presented full seroconversion
128 against RBD, S1 and N for both IgG and IgM were identified. A minority of COVID samples
129 presented only N-reactive IgG and IgM antibodies, testing negative for RBD and S1 (Figure
130 4).

131 **C19BA detects higher amounts of SARS-CoV-2 reactive antibodies in serum samples**
132 **from severe COVID-19 patients compared to mild/moderate COVID-19 patients**

133 We then applied the C19BA assay on an additional set of serum samples obtained at time of
134 hospital admission, corresponding to an independent cohort of patients classified by different
135 clinical outcomes of the disease. These included mild/moderate (n=18) and severe (n=16)
136 cases that tested positive by PCR. Figure 5A shows that levels of anti-RBD and anti-S1 IgG
137 antibodies measured by C19BA were significantly higher in severe COVID cases compared
138 to mild/moderate cases and a control cohort comprising COVID-19 negative samples (n=18).
139 ELISA was performed on the same samples but failed to achieve significant differences
140 between these groups. Figure 5B shows representative patterns of IgG seroconversion in
141 COVID-19 seronegative samples, and mild/moderate and severe COVID-19 cases assayed
142 by C19BA. Sensitivity and specificity values for each antigen analysed by C19BA were
143 calculated by ROC curve analysis of PCR positive and preCOVID samples (Supplementary
144 Figure 4).

145 **C19BA identifies the presence of IgG and IgM on convalescent individuals**

146 We next checked the ability of C19BA of measuring antibody levels on serum samples from
147 convalescent individuals and compared those antibody levels to a seronegative control
148 group. Figure 6A shows that C19BA detects the presence of anti-RBD, anti-S1 and anti-N
149 IgG and IgM antibodies on serum samples from convalescent individuals. The seronegative
150 control group lacked antibody reactivity against RBD and S1, but 4 of 18 samples contained
151 N-reactive IgG antibodies (Figure 6A and 6B). This latest observation is in line with the
152 previous findings on an independent preCOVID cohort (Supplementary Figure 2 and Figure
153 3A, 3B).

154 **Levels of anti-RBD and anti-S1 IgG antibodies measured by C19BA correlate with the**
155 **neutralization capacity of serum samples**

156 We then studied the correlation between anti-SARS-CoV-2 antibody levels and the
157 neutralization capacity of those antibodies. To this end, we tested seronegative (preCOVID,
158 COVID negative) and seropositive (acute and convalescent) samples by C19BA and an
159 ELISA-based inhibition assay that measures the binding of RBD to ACE2. Figure 7A shows
160 that the neutralization capacity of seropositive samples was higher than seronegative
161 samples. We explored correlations between the levels of anti-RBD, anti-S1 and anti-N IgG
162 antibodies measured by C19BA and the inhibition of the interaction RBD/ACE2. RBD and S1
163 reactive antibody levels positively correlate with their inhibition capacity, while the correlation
164 of N-reactive IgG levels was weaker (Figure 7B).

165 **Discussion**

166 Sensitive characterization of humoral responses is critical to control the current pandemic³,
167 because it allows to perform accurate longitudinal serosurveys and epidemiological studies.
168 Moreover, antibodies act as biomarkers for previous exposure and thus can guide
169 vaccination strategies, including booster dosing. Serology assays need to be cost-effective,
170 high-throughput, scalable and easy to implement. In order to fulfil all these requirements, we
171 have developed an assay that combines three viral antigens with superior sensitivity than the
172 ELISAs presented here. The combination of antigens allows for the interrogation of full
173 seroconversion, including the presence of antibodies against the partially redundant and
174 specific RBD and S1 antigens, and the more conserved but strongly immunogenic N
175 protein²⁵. Together, these antigens offer a more specific and rapid platform than conventional
176 assays that use only one viral antigen or require two-step sequential confirmation. In this
177 context, RBD and S1 are specific for anti-SARS-CoV-2 antibodies and are not a source of
178 crossreactivity for antibodies present in samples collected before the pandemic or sera
179 containing antibodies against the spike of other coronaviruses.

180 Another key feature of robust serology assays is sensitivity, which is important to detect low
181 antibody titers. ELISA assays often identify samples with low OD values that are close to the
182 established cut-off, resulting in inconclusive or false positive results. These require repetition
183 of the assay and titration of samples. A previously developed ELISA includes a sequential
184 confirmatory assay with the Spike after positivity against RBD¹². We demonstrate that
185 C19BA presents a superior dynamic range than the ELISA presented here, and an improved
186 limit of detection of low antibody titers. Indeed, C19BA is able to detect the presence of
187 binding antibodies against three different viral antigens at dilutions that were beyond the limit
188 of detection of ELISA.

189 Spike-reactive antibodies have neutralization capacity, even when binding non-RBD Spike
190 epitopes²⁶. On the other hand, N-reactive antibodies are not considered to confer protection
191 and might even be predictive of poor patient outcome in some cases^{27,28}. Levels of anti-RBD

192 and anti-S1 IgG antibodies measured by C19BA on patient samples strongly correlate with
193 the ability of these sera to neutralize the interaction between RBD and ACE2, as expected
194 ²⁹.

195 This superior sensitivity allowed for the identification of low titers of N-reactive antibodies in
196 around 14% (10/68) of Covid-19 seronegative individuals, these antibodies were likely
197 generated as a result of a previous common cold coronavirus infection. This fact raises
198 important concerns about the specificity of the use of N protein for serological assays, given
199 its high homology with N proteins of other coronaviruses. Indeed, several studies reported
200 similar cross-reactivity on serological testing based on N protein during the previous SARS-
201 CoV outbreak in 2004, resulting in false positives^{30,31}.

202 Although most seropositive individuals in the COVID cohort presented antibodies reactive
203 against RBD, S1 and N; a minority of samples only presented N-reactive antibodies. This
204 suggests that these individuals either had antibodies from previous primary infections or
205 mounted fast secondary antibody responses against N after mobilization of memory B cells
206 generated as a result of a previous coronavirus infection. Recently, in a similar fashion, N-
207 specific memory T cells have been also identified in COVID-19 unexposed individuals¹⁸.
208 Together, these data provide evidence that cellular and humoral immune responses against
209 SARS-CoV-2 exist as a result of crossreactivity against the N protein originated by previous
210 coronavirus infections. The impact of these pre-existing T cell and antibody responses in the
211 control and pathogenesis of COVID-19 requires further investigation.

212 In summary, we have developed a novel multiplexed method with higher sensitivity than
213 traditional serology assays, using a triple combination of antigens that exploits the specificity
214 of the Spike and RBD together with the less-specific N protein for the detection of antibodies
215 against SARS-CoV-2.

216 **Methods**

217 **Serum samples.** Serum samples corresponding to preCOVID and acute COVID individuals
218 were provided by the Basque Biobank (www.biobancovasco.org) after approval from the
219 corresponding ethics committee (CEIC-E 20-26, 1-2016). All participants in the study
220 provided informed consent and were anonymized. The serum samples corresponding to the
221 acute COVID cohort (43 patients presenting COVID-19 symptomatology and diagnosed by
222 PCR) were obtained at time of hospital admission. The preCOVID cohort (50 serum
223 samples) was obtained during the yearly medical check-up of the working population of the
224 Basque Country in 2018-2019 in collaboration with Osarten Kooperatiba Elkartea from
225 Mondragon Corporation. Additional serum samples from negative controls (n=18) and
226 independent COVID-19 cohorts confirmed by PCR were obtained after written informed
227 consent and approval by the Cantabria Ethics Committee (CEIm Code: 2020.167). Serum
228 samples from 34 patients with active infection were obtained at time of hospital admission,
229 and samples from 20 convalescent patients were obtained one month after recovery from
230 COVID-19. Severity of the disease was defined as mild/moderate (n=18) or severe (n=16).
231 Severity was classified based on admission to the intensive care unit (ICU), and oxygen
232 levels as defined previously³².

233 **Microbead coating.** PMMA (polymethyl methacrylate) 8.2 μm microbeads coated with
234 streptavidin were purchased from PolyAn (Cat#10652009). Each type of microbead
235 presented a different fluorescence intensity (Red4 dye, Excitation: 590-680 nm/Emission:
236 660-780 nm). First, microbeads were washed with cold PBS pH 7.2 (Gibco Cat#14190-094)
237 by centrifugation at 2000 rpm for 5 min and resuspended in PBS. Then, biotinylated
238 recombinant RBD, S1 and N (Acrobiosystems Cat#SPD-C82E9, Cat#S1N-C82E8 and
239 Cat#NUN-C81Q6, respectively) were added to the tubes (RBD at 11 $\mu\text{g}/\text{mL}$, S1 at 30 $\mu\text{g}/\text{mL}$,
240 N at 19,5 $\mu\text{g}/\text{mL}$) and kept at 4°C on rotating head over tail for an hour, protected from light.
241 Positive control beads were coated with biotinylated human IgG (Novus Biologicals
242 Cat#NBP1-96855) and IgM (Novus Biologicals Cat#NBP1-96989) on the same microbead at

243 15 µg/mL each. Negative control beads were not coated with protein. After the coupling
244 reaction, microbeads were washed three times with PBS. Then, D-biotin (2 µM) (Sigma-
245 Aldrich Cat#8512090001) was added and incubated for 15 min at room temperature (RT) to
246 inactivate residual streptavidin. After three additional washes, equal amounts of each
247 microbead were combined in the same vial.

248 **C19BA assay.** Antigen-coupled microbeads were added to protein LoBind 1.5 mL
249 Eppendorf tubes (Eppendorf Cat#525-0133) in a volume of 50 µL of PBS containing a total
250 of 5000-6000 beads. After centrifugation (2000 rpm, 5 min), microbeads were resuspended
251 with 100 µL of pre-diluted (PBS) serum samples or serially diluted commercial antibodies
252 against RBD (GenScript Cat#A02038) or N (Acrobiosystems Cat#NUN-S41) starting from a
253 1 mg/mL concentration. Negative control samples were prepared with PBS. After a 30
254 minute incubation (RT protected from light), samples were washed three times in PBS.
255 Secondary antibodies were diluted in 100 µL of PBS containing 5% FBS: anti-human IgG-PE
256 (1:50) (Clone G18-145, BD Biosciences Cat#555787) and anti-human IgM-BV421 antibodies
257 (1:1000) (Clone G20-127, BD Biosciences Cat#555783). The mix was incubated with the
258 samples for 15 min at RT protected from light. One final wash was performed, and
259 microbeads were resuspended in 200 µL of PBS supplemented with 5% FBS for acquisition.
260 At least 600 events for each type of microbead were acquired in a FACSymphony flow
261 cytometer (BD Biosciences) and geometric mean fluorescence intensities (gMFI) were
262 obtained. Results were analyzed using FlowJo version 10 (BD Biosciences).

263 **ELISA.** The protocol was adapted from a previously established immunoassay¹³. Briefly, 96-
264 well ELISA plates (Nunc Maxisorp Cat#44-2404-21) were coated overnight at 4°C with 50 µL
265 of biotinylated RBD, S1 or N protein (Acrobiosystems), at 2 µg/mL (for RBD and S1) or 1.4
266 µg/mL (N) in PBS (Gibco). In some cases, recombinant S1 protein from human
267 coronaviruses HCoV-NL63 or HCoV-229E (Sino Biological Inc., Cat#40600-V08H, 40601-
268 V08H) were used to coat the plates. Then, the coating solution was removed and plates
269 were blocked with 3% non-fat milk in PBST (PBS plus 0.1% Tween-20) for 1 hour at RT.

270 Serum samples were pre-diluted in 1% non-fat milk in PBST, and incubated for 2 hours at
271 RT. After three washes with 250 μ L of PBST in a plate washer (Biotek), each well was
272 incubated with an anti-human IgG-horseradish peroxidase (HRP) conjugated secondary
273 antibody (1:5000) (GenScript Cat#A01854) or anti-human IgM-HRP (Novus Biologicals
274 Cat#NBP1-75014) for 1 hour at RT. Plates were washed three times with PBST, and 100 μ L
275 of TMB substrate (Thermo Scientific Cat#34021) were added to each well, incubated for 2
276 min and the reaction was stopped with 50 μ L of stop solution (Thermo Scientific Cat#N600).
277 The optical density (OD) was measured at 450 nm in a VictorNivo multimode plate reader
278 (PerkinElmer).

279 **Neutralization assay.** Binding of RBD to recombinant ACE2 was measured by a
280 commercial surrogate virus neutralization test (sVNT) (cPass™ SARS-CoV-2 Neutralization
281 Antibody Detection Kit, Genscript)³³. The percentage of inhibition was calculated with the
282 following formula: $(1 - \text{sample OD value} / \text{average preCOVID OD value}) \times 100$. Pearson
283 correlation analyses between gMFI values obtained by C19BA and percentage of inhibition
284 obtained by the neutralization assay for anti-RBD, anti-S1 and anti-N IgG antibodies were
285 calculated using Prism 8 (GraphPad) considering a 95% confidence interval.

286 **Statistics.** To calculate the sample ODs and gMFIs, the values corresponding to the
287 negative controls were subtracted from all samples. The AUC values were calculated as
288 described in Amanat et al.¹². Briefly, the background was set at 0.11 for each sample and
289 AUC values were calculated using Prism 8 (GraphPad). The resulting values were divided
290 by 100 and those that were below 1 were assigned a value of 0.5 for plotting purposes.
291 Statistical analyses comparing different cohorts were performed with an unpaired two-tailed
292 Student's t-test. Data were analyzed using Prism 8 (GraphPad). Phylogram generated from
293 the FASTA alignment file was performed using FastTree (<https://www.genome.jp/>). Receiver
294 operating characteristic (ROC) curves and the corresponding AUC values were computed
295 using the pROC R package (v.1.17.0.1)³⁴. The values that maximized the Youden index
296 were selected as the cut-off for reporting sensitivity and specificity values.

297 **References**

- 298 1 Zhou, P. *et al.* A pneumonia outbreak associated with a new coronavirus of probable
299 bat origin. *Nature* **579**, 270-273, doi:10.1038/s41586-020-2012-7 (2020).
- 300 2 Lee, C. Y., Lin, R. T. P., Renia, L. & Ng, L. F. P. Serological Approaches for COVID-
301 19: Epidemiologic Perspective on Surveillance and Control. *Front Immunol* **11**, 879,
302 doi:10.3389/fimmu.2020.00879 (2020).
- 303 3 Theel, E. S. *et al.* The Role of Antibody Testing for SARS-CoV-2: Is There One? *J*
304 *Clin Microbiol* **58**, doi:10.1128/JCM.00797-20 (2020).
- 305 4 GeurtsvanKessel, C. H. *et al.* An evaluation of COVID-19 serological assays informs
306 future diagnostics and exposure assessment. *Nat Commun* **11**, 3436,
307 doi:10.1038/s41467-020-17317-y (2020).
- 308 5 Bryant, J. E. *et al.* Serology for SARS-CoV-2: Apprehensions, opportunities, and the
309 path forward. *Sci Immunol* **5**, doi:10.1126/sciimmunol.abc6347 (2020).
- 310 6 Zhang, W. *et al.* Molecular and serological investigation of 2019-nCoV infected
311 patients: implication of multiple shedding routes. *Emerg Microbes Infect* **9**, 386-389,
312 doi:10.1080/22221751.2020.1729071 (2020).
- 313 7 Amanat, F. & Krammer, F. SARS-CoV-2 Vaccines: Status Report. *Immunity* **52**, 583-
314 589, doi:10.1016/j.immuni.2020.03.007 (2020).
- 315 8 Zost, S. J. *et al.* Rapid isolation and profiling of a diverse panel of human monoclonal
316 antibodies targeting the SARS-CoV-2 spike protein. *Nat Med*, doi:10.1038/s41591-
317 020-0998-x (2020).
- 318 9 Shang, J. *et al.* Structural basis of receptor recognition by SARS-CoV-2. *Nature* **581**,
319 221-224, doi:10.1038/s41586-020-2179-y (2020).
- 320 10 Walls, A. C. *et al.* Structure, Function, and Antigenicity of the SARS-CoV-2 Spike
321 Glycoprotein. *Cell* **181**, 281-292 e286, doi:10.1016/j.cell.2020.02.058 (2020).
- 322 11 Chi, X. *et al.* A neutralizing human antibody binds to the N-terminal domain of the
323 Spike protein of SARS-CoV-2. *Science*, doi:10.1126/science.abc6952 (2020).
- 324 12 Amanat, F. *et al.* A serological assay to detect SARS-CoV-2 seroconversion in
325 humans. *Nat Med*, doi:10.1038/s41591-020-0913-5 (2020).
- 326 13 Stadlbauer, D. *et al.* SARS-CoV-2 Seroconversion in Humans: A Detailed Protocol
327 for a Serological Assay, Antigen Production, and Test Setup. *Curr Protoc Microbiol*
328 **57**, e100, doi:10.1002/cpmc.100 (2020).
- 329 14 Premkumar, L. *et al.* The receptor binding domain of the viral spike protein is an
330 immunodominant and highly specific target of antibodies in SARS-CoV-2 patients.
331 *Sci Immunol* **5**, doi:10.1126/sciimmunol.abc8413 (2020).

- 332 15 Watanabe, Y., Allen, J. D., Wrapp, D., McLellan, J. S. & Crispin, M. Site-specific
333 glycan analysis of the SARS-CoV-2 spike. *Science* **369**, 330-333,
334 doi:10.1126/science.abb9983 (2020).
- 335 16 Ni, L. *et al.* Detection of SARS-CoV-2-Specific Humoral and Cellular Immunity in
336 COVID-19 Convalescent Individuals. *Immunity* **52**, 971-977 e973,
337 doi:10.1016/j.immuni.2020.04.023 (2020).
- 338 17 Ju, B. *et al.* Human neutralizing antibodies elicited by SARS-CoV-2 infection. *Nature*,
339 doi:10.1038/s41586-020-2380-z (2020).
- 340 18 Le Bert, N. *et al.* SARS-CoV-2-specific T cell immunity in cases of COVID-19 and
341 SARS, and uninfected controls. *Nature*, doi:10.1038/s41586-020-2550-z (2020).
- 342 19 Grifoni, A. *et al.* Targets of T Cell Responses to SARS-CoV-2 Coronavirus in
343 Humans with COVID-19 Disease and Unexposed Individuals. *Cell* **181**, 1489-1501
344 e1415, doi:10.1016/j.cell.2020.05.015 (2020).
- 345 20 Mateus, J. *et al.* Selective and cross-reactive SARS-CoV-2 T cell epitopes in
346 unexposed humans. *Science*, doi:10.1126/science.abd3871 (2020).
- 347 21 Lisboa Bastos, M. *et al.* Diagnostic accuracy of serological tests for covid-19:
348 systematic review and meta-analysis. *BMJ* **370**, m2516, doi:10.1136/bmj.m2516
349 (2020).
- 350 22 Duong, Y. T., Wright, C. G. & Justman, J. Antibody testing for coronavirus disease
351 2019: not ready for prime time. *BMJ* **370**, m2655, doi:10.1136/bmj.m2655 (2020).
- 352 23 Morgan, E. *et al.* Cytometric bead array: a multiplexed assay platform with
353 applications in various areas of biology. *Clin Immunol* **110**, 252-266,
354 doi:10.1016/j.clim.2003.11.017 (2004).
- 355 24 Leng, S. X. *et al.* ELISA and multiplex technologies for cytokine measurement in
356 inflammation and aging research. *J Gerontol A Biol Sci Med Sci* **63**, 879-884,
357 doi:10.1093/gerona/63.8.879 (2008).
- 358 25 Timani, K. A. *et al.* Cloning, sequencing, expression, and purification of SARS-
359 associated coronavirus nucleocapsid protein for serodiagnosis of SARS. *J Clin Virol*
360 **30**, 309-312, doi:10.1016/j.jcv.2004.01.001 (2004).
- 361 26 Liu, L. *et al.* Potent neutralizing antibodies directed to multiple epitopes on SARS-
362 CoV-2 spike. *Nature*, doi:10.1038/s41586-020-2571-7 (2020).
- 363 27 Yasui, F. *et al.* Prior immunization with severe acute respiratory syndrome (SARS)-
364 associated coronavirus (SARS-CoV) nucleocapsid protein causes severe pneumonia
365 in mice infected with SARS-CoV. *J Immunol* **181**, 6337-6348,
366 doi:10.4049/jimmunol.181.9.6337 (2008).
- 367 28 Atyeo, C. *et al.* Distinct early serological signatures track with SARS-CoV-2 survival.
368 *Immunity*, doi:10.1016/j.immuni.2020.07.020 (2020).

- 369 29 Robbiani, D. F. *et al.* Convergent antibody responses to SARS-CoV-2 in
370 convalescent individuals. *Nature* **584**, 437-442, doi:10.1038/s41586-020-2456-9
371 (2020).
- 372 30 Woo, P. C. *et al.* False-positive results in a recombinant severe acute respiratory
373 syndrome-associated coronavirus (SARS-CoV) nucleocapsid enzyme-linked
374 immunosorbent assay due to HCoV-OC43 and HCoV-229E rectified by Western
375 blotting with recombinant SARS-CoV spike polypeptide. *J Clin Microbiol* **42**, 5885-
376 5888, doi:10.1128/JCM.42.12.5885-5888.2004 (2004).
- 377 31 Patrick, D. M. *et al.* An Outbreak of Human Coronavirus OC43 Infection and
378 Serological Cross-reactivity with SARS Coronavirus. *Can J Infect Dis Med Microbiol*
379 **17**, 330-336, doi:10.1155/2006/152612 (2006).
- 380 32 Lucas, C. *et al.* Longitudinal analyses reveal immunological misfiring in severe
381 COVID-19. *Nature* **584**, 463-469, doi:10.1038/s41586-020-2588-y (2020).
- 382 33 Tan, C. W. *et al.* A SARS-CoV-2 surrogate virus neutralization test based on
383 antibody-mediated blockage of ACE2-spike protein-protein interaction. *Nat*
384 *Biotechnol* **38**, 1073-1078, doi:10.1038/s41587-020-0631-z (2020).
- 385 34 Robin, X. *et al.* pROC: an open-source package for R and S+ to analyze and
386 compare ROC curves. *BMC Bioinformatics* **12**, 77, doi:10.1186/1471-2105-12-77
387 (2011).

388 **Acknowledgements**

389 We thank Petros Tyrakis and Iván Martínez-Forero for critical reading and editing of the
390 manuscript. Grant support: Support was provided by the Severo Ochoa Excellence
391 Accreditation from MCIU (SEV-2016-0644) and the SPRI I+D COVID-19 fund (Gobierno
392 Vasco). Personal fellowships: A.A.V. (La Caixa Inphinit), A.B. (AECC Bizkaia), A.G.D.R
393 (Bikaintek), A.P. (Ramón y Cajal), B.J.L. (Gob. Vasco) and E.P.F. (Juan de la Cierva-
394 Formación). M.L.M.C. acknowledges RTC2019-007125-1, DTS20/00138, SAF2017-87301-
395 R, and BBVA UMBRELLA project. M.L.H. acknowledges the ISCIII for grant COV20-0170
396 and the Government of Cantabria for grant 2020UIC22-PUB-0019. O.M.-J.M.M. and
397 N.G.A.A. acknowledge the Agencia Estatal de Investigación (Spain) for grants CTQ2015-
398 68756-R, RTI2018-101269-B-I00 and RTI2018-095700-B-I00, respectively. A.P. has
399 received grant funding from the European Research Council (ERC), grant agreement
400 number 804236 (Horizon 2020), and the FERRO Foundation.

401 **Author contributions**

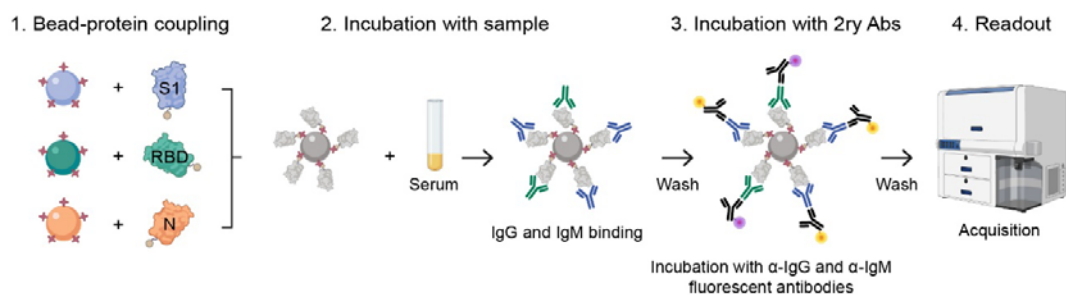
402 A.P. conceived and administered the project. L.E.M. and A.B. performed all experiments and
403 analysed data. A.B., L.E.M., N.G.A.A. R.G.R. and E.P.F. performed computational and
404 statistical analyses. A.G.D.R., S.Y.L., B.J.L. and A.A.V. contributed ideas. O.M., J.M.M.,
405 C.B., M.B., N.E., M.L.M.C and M.L-H provided patient samples. A.P. wrote the manuscript
406 with help from all co-authors.

407 **Competing interests statement**

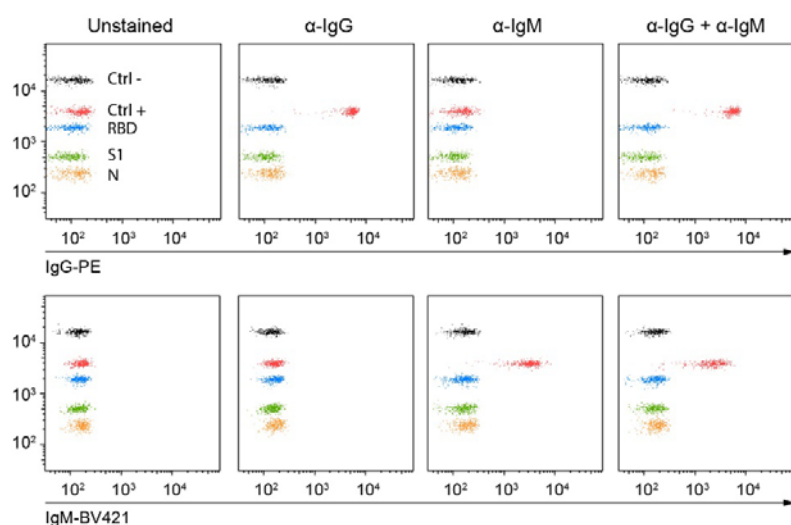
408 The authors declare no competing interests.

Figure 1

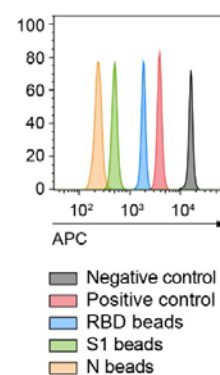
a



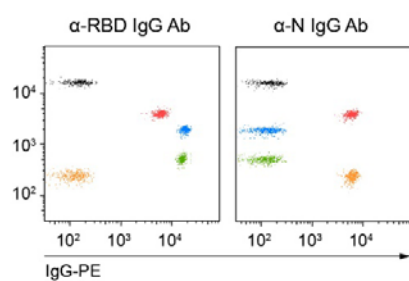
b



c



d

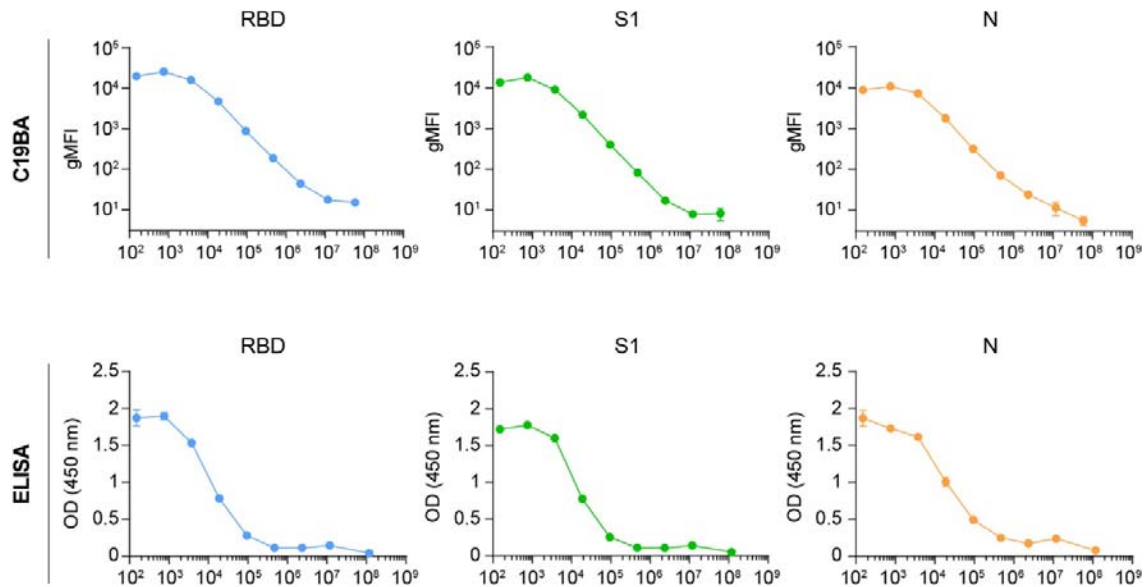


409

410 **Figure 1. Workflow and performance of C19BA. (A)** Overview of the detection of SARS-
411 CoV-2 seroconversion by flow cytometric bead array. Streptavidin-coated microbeads with
412 different fluorescence intensities are conjugated with recombinant biotinylated viral antigens
413 (RBD, S1 and N) and mixed and incubated with prediluted serum samples together with
414 control beads. After incubation, microbeads are washed and stained with anti-human IgG

415 and IgM secondary antibodies, washed and acquired on a flow cytometer for downstream
416 analysis. **(B)** Dot plots showing the staining patterns of positive (red) and negative (black)
417 control beads with secondary anti-IgG-PE, anti-IgM-BV421 or both. The signal
418 corresponding to IgG-PE (top) and IgM-BV421 (bottom) is shown for each column. **(C)**
419 Histogram showing the distribution of the microbeads based on their intrinsic fluorescence
420 on the APC channel. Each colour represents the coating for each microbead. **(D)**
421 Representative dot plots showing the specificity of the staining pattern of recombinant anti-
422 RBD IgG (left) or anti-N IgG (right) antibodies.

Figure 2



423

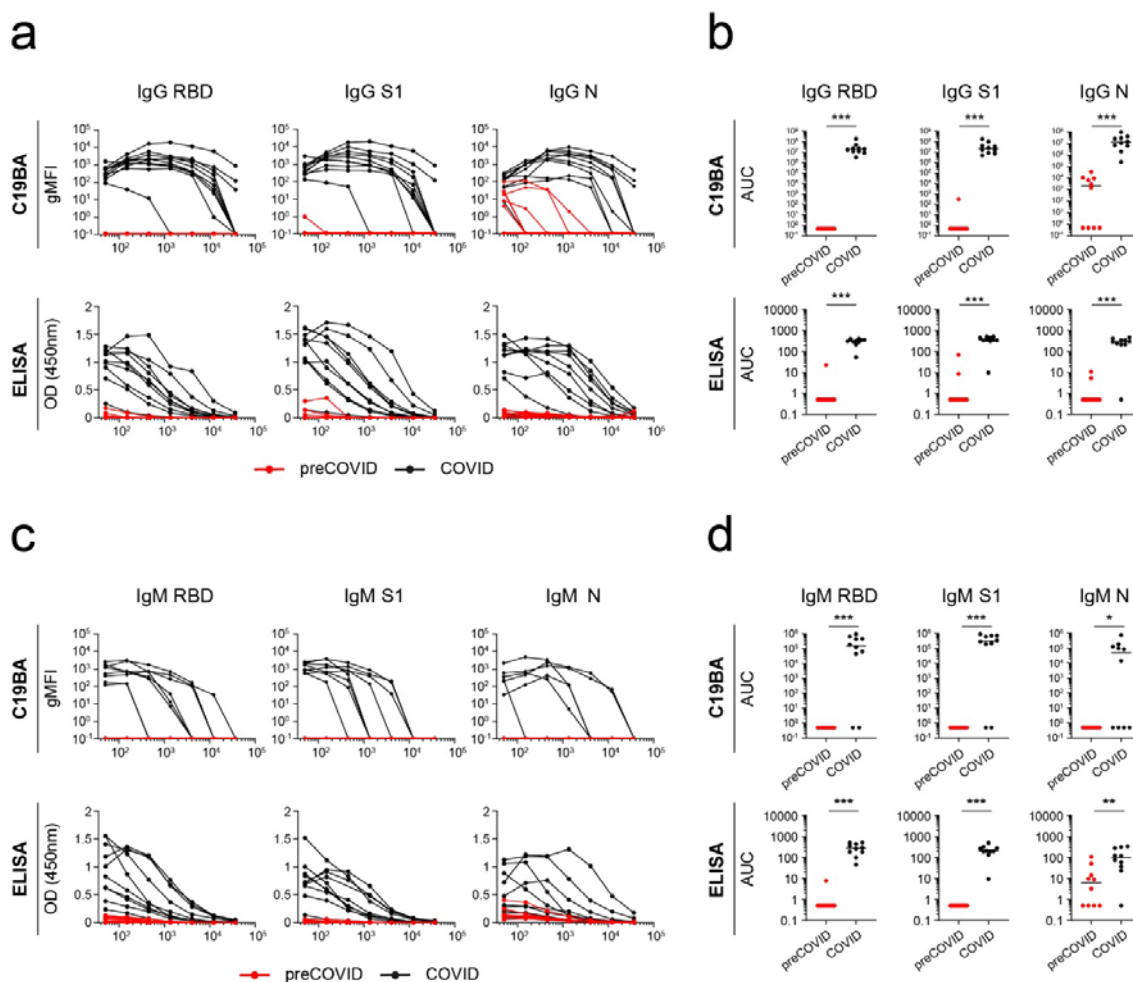
424 **Figure 2. C19BA has superior sensitivity and greater dynamic range than ELISA.**

425 Comparison of the titration of anti-RBD (blue and green) and anti-N (orange) IgG antibodies

426 against recombinant RBD, S1 and N proteins by C19BA (top) and ELISA (bottom). The

427 mean value of two replicates is shown, error bars represent SD.

Figure 3



428

429 **Figure 3. Identification of SARS-CoV-2 IgG and IgM seroconversion by C19BA. (A)**

430 Titration curves of the reactivity of individual serum samples against RBD, S1 and N proteins

431 measured by flow cytometry against IgG by C19BA (top) and ELISA (bottom) for each

432 cohort: preCOVID (red, n=10) and COVID (black, n=10). COVID serum samples were

433 obtained at time of hospital admission (PCR+) (B) AUC values for the experiment shown in

434 (A). (C) Titration curves of the reactivity of individual serum samples against RBD, S1 and N

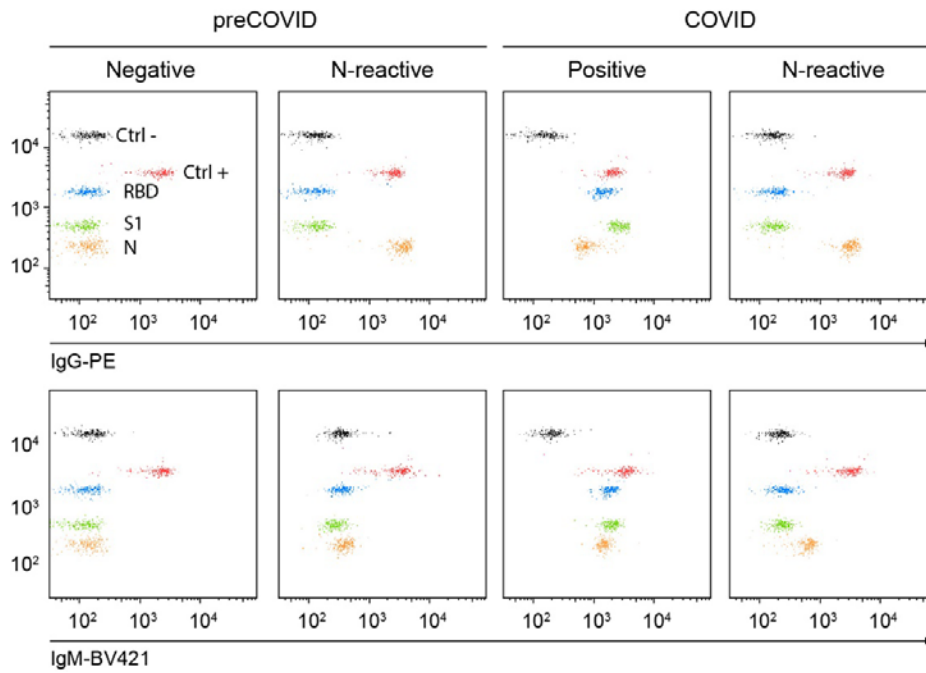
435 proteins against IgM by C19BA (top) and ELISA (bottom). (D) AUC values for the experiment

436 shown in (C). Statistical analyses were performed using an unpaired two-tailed Student's t-

437 test. Asterisks represent p values (***) p < 0.001, (*) p < 0.05, ns: not significant). Horizontal lines

438 represent median values.

Figure 4



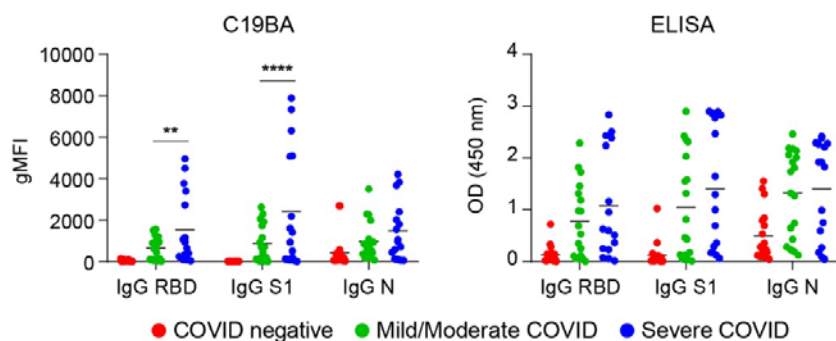
439

440 **Figure 4. C19BA reveals different serology patterns in preCOVID and COVID samples**
441 **collected at time of hospital admission (PCR+).** Dot plots showing IgG (top) and IgM
442 (bottom) reactivity against RBD, S1 and N for representative preCOVID and COVID
443 samples.

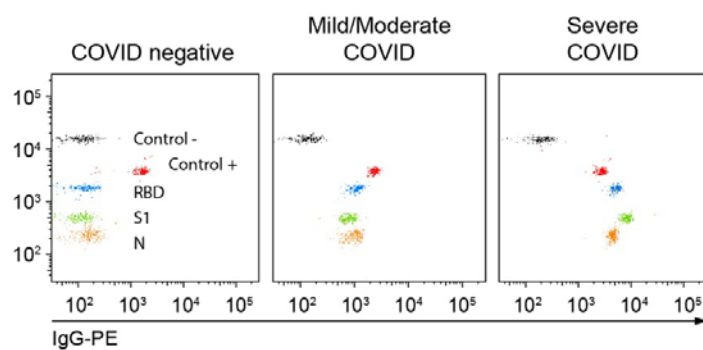
444

Figure 5

a



b

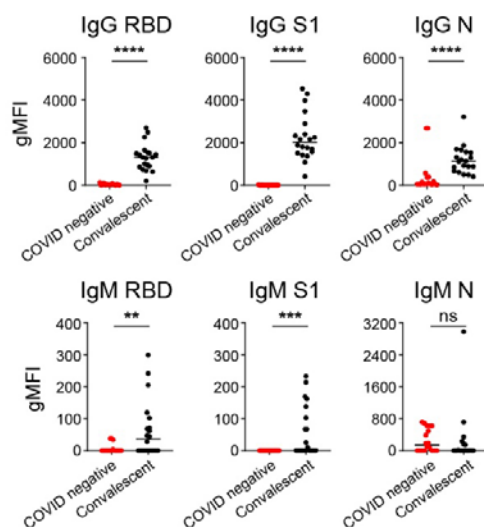


445

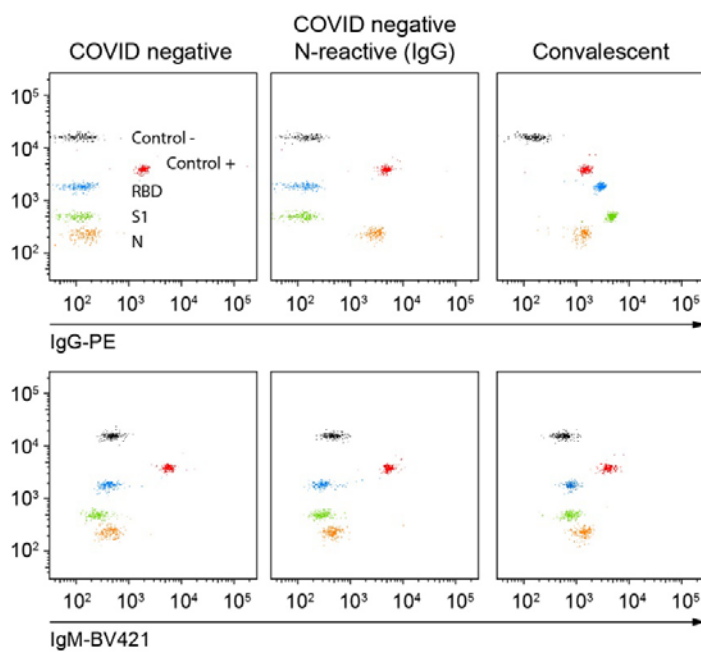
446 **Figure 5. Severe Covid-19 patients present higher levels of anti-spike IgG antibodies**
447 **compared to moderate Covid-19 patients. (A)** gMFI values obtained by C19BA (left) and
448 OD values obtained by ELISA (right) corresponding to levels of IgG against RBD, S1 and N
449 for the indicated cohorts. **(B)** Representative dot plots obtained by C19BA showing IgG
450 levels for COVID negative, mild/moderate COVID and severe COVID serums obtained from
451 PCR+ individuals at time of hospital admission. Statistical analyses were performed using
452 two-way ANOVA. Asterisks represent p values (**** p<0.0001, * p<0.05). Horizontal lines
453 represent median values.

Figure 6

a



b

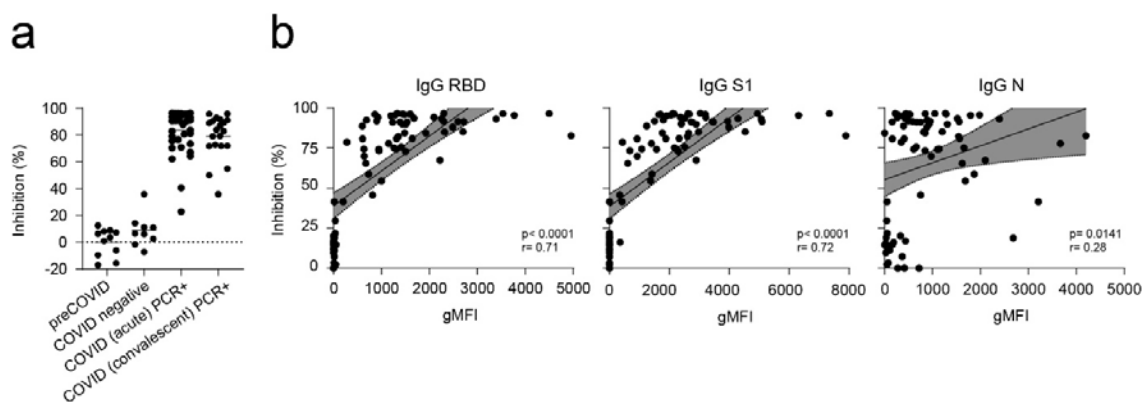


454

455 **Figure 6. C19BA identifies IgG and IgM seroconversion in a cohort of samples from**
456 **convalescent donors, and the presence of N-reactive IgG antibodies in Covid-**
457 **seronegative samples. (A) Serological responses against RBD, S1 and N measured by**
458 **C19BA on serum samples from convalescent patients after at least one month of disease**

459 onset, IgG (top) and IgM (bottom) are shown. **(B)** Representative dot plots obtained by
460 C19BA showing IgG (top) and IgM (bottom) levels, as indicated. Statistical analyses were
461 performed using an unpaired two-tailed Student's t-test. Asterisks represent p values (****
462 $p < 0.0001$, *** $p < 0.001$, ** $p < 0.01$). Horizontal lines represent median values.

Figure 7



463

464 **Figure 7. Levels of anti-RBD and anti-S1 IgG antibodies measured by C19BA correlate**
465 **with neutralization capacity of serum samples. (A)** Neutralization assay performed on
466 samples from different cohorts of individuals as indicated, including healthy and seropositive
467 donors. **(B)** Correlation of gMFI values obtained by C19BA and % Inhibition obtained by the
468 neutralization assay for anti-RBD IgG (left), anti-S1 IgG (middle), and anti-N IgG (right). (n=
469 77). Pearson correlation coefficients (r) and their corresponding p values are shown.